Synthesis of III–V Semiconductors by Solid-State Metathesis

Randolph E. Treece,† Gerald S. Macala,† Lin Rao,† Deanna Franke,‡ Hellmut Eckert,‡ and Richard B. Kaner*,†

Department of Chemistry and Biochemistry and Solid State Science Center, University of California, Los Angeles, California 90024-1569, and Department of Chemistry, University of California, Santa Barbara, California 93106

Received July 22, 1992

Solid-state precursor reactions have been investigated as a general synthetic route to binary III–V (13–15) compounds. The generic reaction scheme $MX_3 + Na_3Pn \rightarrow MPn + 3\ NaX$ (M = Al, Ga, In; X = F, Cl, I; Pn = pnictogen = P, As, Sb) has been used to prepare crystalline powders of the III–V semiconductors. The reaction mixtures can be either heated in sealed tubes or ignited with a hot filament, and the byproduct salts are simply removed by washing with an appropriate solvent. The ignited reactions are self-propagating and highly exothermic, owing to the formation of 3 mol of sodium halide. Products from both types of reactions have been characterized by powder X-ray diffraction, scanning electron microscopy, energy dispersive spectroscopy, and solid-state NMR. In some cases, the products of the ignited solid-state metathesis (SSM) reactions differ from those of the sustained heating reactions. These differences provide clues as to reaction pathways in the solid-state precursor reactions.

Introduction

The III–V (13–15) compound semiconductors are well-known electronic and optoelectronic materials.[1] Early synthetic approaches to 13–15 materials resemble traditional solid-state chemistry methods.[2,3] The respective elements are heated (usually above 1000 °C) in evacuated, sealed ampules for long durations (days to weeks). The products are frequently inhomogeneous, the processes often incomplete, and reaction with the fused silica ampules is common. It is, therefore, necessary to intermittently remove and pulverize the samples during the heating process. In addition, the high vapor pressures of phosphorus and arsenic above their respective compounds at elevated temperatures can lead to P- and As-deficient compounds.

In order to overcome the problems of traditional high-temperature elemental reactions, alternative synthetic methods have been devised. One approach is to introduce the phosphorus as a metal phosphide precursor.[4] A solid-state elimination reaction between aluminum (or gallium, or indium) and Zn_3P_2 produced AlP (or GaP, or InP) after heating the mixed powders for 5 h at 850 °C. The zinc byproduct was removed from the AlP product by vapor transport in a temperature gradient. Another route utilized excess metal halides in combination with elemental pnictogens (group 13 elements).[5,6] The metal halides (MX_y where y = 1–3) were introduced to the reaction mixture either intact or made *in situ* by allowing the metal and the halide (usually I_2) to prereact at temperatures below where the metal would combine with the pnictide. The 13–15 compounds could often be prepared at less than 600 °C in fewer than 12 h, with the excess metal halide removed by vapor transport. Other synthetic approaches include precipitating amorphous 13–15 materials from solution[7] and decomposing single-source precursors to yield bulk powders.[8] In addition, synthetic routes to a variety of materials based on solid-state metathesis (SSM) reactions have been described. SSM reactions of the type AB + CD → AD + CB between metal halides (MX_y where y = 2–6) and alkali-metal nonmetalides (Na_2S, Na_3P, Li_3N, etc.) have been used to produce layered transition-metal dichalcogenides (MoS_2, WSe_2, etc.),[9–12] magnetic rare-earth-element compounds (GdP, GdAs, etc.),[13] and refractory materials (ZrN, $MoSi_2$, etc.)[12,14,15] These reactions are self-sustaining and generally yield polycrystalline materials.

Self-sustaining reactions have been exploited for many years. The Thermite process is a well-known self-sustaining reaction in which mixtures of ferric oxide and aluminum powder packed in the gap between adjacent rails are ignited with local heating. The reaction takes off, forming metallic iron and alumina. The driving

† University of California, Los Angeles.
‡ University of California, Santa Barbara.

(1) (a) Sze, S. M. *Physics of Semiconductor Devices*, 2nd ed.; John Wiley and Sons: New York, 1981. (b) Streetman, B. G. *Solid State Electronic Devices*, 3rd ed.; Prentice Hall: Englewood Cliffs, NJ, 1990. (c) Grovenor, C. R. M. *Microelectronic Materials*; Adam Hilger: Philadelphia, PA 1989.
(2) An early review of synthetic approaches to 13–15 compounds is presented in: *Compound Semiconductors*; Willardson, R. K., Goering, H. L., Eds.; Reinhold: New York, 1962; Vol. I.
(3) Novel synthetic approaches to 13–15 and other compounds are presented in: *Preparative Methods in Solid State Chemistry*; Hagenmuller, P., Ed.; Academic Press: New York, 1972.
(4) Addamiano, A. *J. Am. Chem. Soc.* **1960**, *82*, 1537.
(5) (a) Antell, G. R.; Effer, D. *J. Electrochem. Soc.* **1959**, *106*, 509. (b) Effer, D.; Antell, G. R. *J. Electrochem. Soc.* **1960**, *107*, 252.
(6) Kwestroo, W. Preparation of Chalcogenides and Pnyctides at Low Temperatures. In *Preparative Methods in Solid State Chemistry*, Hagenmuller, P., Ed.; Acedemic Press: New York, 1972; pp 563–574.
(7) (a) Cumberbatch, T. J.; Putnis, A. *Mater. Res. Soc. Symp. Proc.* **1990**, *164*, 129. (b) Byrne, E. K.; Parkanyi, L.; Theopold, K. H. *Science (Washington, D.C.)* **1988**, *241*, 332. (c) Lawrence, D. W. U.S. Pat. No. 4,798,701, Jan 17, 1989.
(8) (a) Wells, R. L.; Pitt, C. G.; McPhail, A. T.; Purdy, A. P.; Shafieezad, S.; Hallock, R. B. *Chem. Mater.* **1989**, *1*, 4. (b) Wells et al. have also discussed routes to AlAs and InAs, as well as GaAs: Wells, R. L.; Pitt, C. G.; McPhail, A. T.; Purdy, A. P.; Shafieezad, S.; Hallock, R. B. *Mater. Res. Soc. Symp. Proc.* **1989**, *131*, 45. (c) Wells, R. L.; Hallock, R. B.; McPhail, A. T.; Pitt, C. G.; Johansen, J. D. *Chem. Mater.* **1991**, *3*, 381. (d) Cowley, A. H.; Harris, P. R.; Jones, R. A.; Nunn, C. M. *Organometallics* **1991**, *10*, 652. (e) Cowley et al. have also deposited films of GaAs and InP from single-source precursors, such as $[Me_2Ga(\mu\text{-}t\text{-}Bu_2As)]_2$ (used to prepare GaAs): Cowley, A. H.; Benac, B. L.; Ekerdt, J. G.; Jones, R. A.; Kidd, K. B.; Lee, J. Y.; Miller, J. E. *J. Am. Chem. Soc.* **1988**, *110*, 6248–6249.
(9) (a) Bonneau, P. R.; Shibao, R. K.; Kaner, R. B. *Inorg. Chem.* **1990**, *29*, 2511. (b) Bonneau, P. R.; Jarvis, R. F., Jr.; Kaner, R. B *Nature* **1991**, *349*, 510. (c) Bonneau, P. R.; Jarvis, R. F., Jr.; Kaner, R. B. *Inorg. Chem.* **1992**, *31*, 2127.
(10) Bonneau, P. R.; Wiley, J. B.; Kaner, R. B. *Inorg. Synth.*, in press.
(11) Wiley, J.; Bonneau, P.; Treece, R.; Jarvis, R., Jr.; Gillan, E.; Rao, L.; Kaner, R. B. In *Supramolecular Architecture: Tailoring Structure and Function of Extended Assemblies*; Bein, T., Ed.; ACS Symposium Series No. 499; American Chemical Society: Washington, DC, 1992.
(12) Wiley, J. B.; Kaner, R. B. *Science (Washington, DC)* **1992**, *255*, 1093–1097.
(13) Treece, R. E.; Kaner, R. B. *Chem. Mater.*, submitted for publication.
(14) Treece, R. E; Gillan, E. G.; Jacubinas, R. M.; Wiley, J. B.; Kaner, R. B. Better Ceramics Through Ceramics V. *Mater. Res. Soc. Symp. Proc.* **1992**, *271*, 169–174.
(15) Kaner, R.; Bonneau, P.; Gillan, E.; Wiley, J.; Jarvis, R., Jr.; Treece, R. U.S. Pat. No. 5,110,768, May 5, 1992.

0020-1669/93/1332-2745$04.00/0

force behind the Thermite process is the formation of Al_2O_3 ($\Delta H_{reacn} = -204$ kcal/mol of Al).[16] The idea of using high ΔH's of reaction as the primary heat source to form products was developed by Soviet researchers over 25 years ago. "Self-propagating high-temperature synthesis" (SHS) was the term used for combustion reactions between compacted mixtures of fine elemental powders. SHS reactions are now capable of producing intermetallics, borides, silicides, carbides, nitrides, and many other important materials.[17] An important consideration in SHS reactions is the adiabatic temperature, T_{ad}. This is the theoretical maximum temperature to which the products may be raised in any combustion event, given the heat of reaction and the thermodynamic functions of heat capacities and enthalpies of fusion, vaporization, and any structural transformation(s).[18] Values of T_{ad} can vary in SHS reactions from less than 1100 to greater than 5000 K.

Recently, we reported a rapid SSM synthesis of polycrystalline GaP and GaAs.[19] The X-ray-pure materials were produced in self-sustaining exchange reactions between mixtures of GaI_3 and Na_3P or Na_3As, which were ignited with a hot filament. Here we report a more general solid-state precursor route applicable to all of the 13–15 materials, evaluate the quality of these products by powder X-ray diffraction, chemical analysis, and solid-state NMR, and discuss a possible mechanistic pathway for the ignited SSM reactions.

Experimental Section

Precursor Preparation. Metal iodide (MI_3) precursors were made from the elements at about 300 °C in sealed Pyrex ampules and then purified by direct vapor transport in a 300 °C–room temperature gradient. Indium fluoride (InF_3) was purchased from Johnson Matthey/Alfa (96%) and purified by reaction with fluorine at 300 °C for 3 h. Gallium fluoride (GaF_3) and gallium chloride ($GaCl_3$) were purchased from Johnson Matthey/Aesar (99.999%) and used as received. The sodium pnictides (Na_3X) were prepared by heating stoichiometric amounts of the constituent elements in sealed Pyrex ampules for 5 h at 500 °C, opening the tube and grinding the contents in a He-filled drybox, reloading and sealing the contents under vacuum, and reheating for an additional 5 h at 500 °C. (*CAUTION*! The sodium pnictides are toxic and highly reactive to air and water.)

Metathesis Reactions. The precursor manipulations were carried out in a He-filled drybox where the metal halide and sodium pnictide were ground individually, mixed in equimolar quantities, and then either (method 1) sealed under vacuum in clean, dry tubes and heated to a set temperature or (method 2) ignited with a hot filament in a bomb similar to those used in calorimetry experiments.[10] (In some cases the reactions self-detonate on mixing or upon exposure to a vacuum; therefore, caution should be exercised in working with these precursor mixtures. Cooling the sample tube while on the vacuum line prevents accidental ignition of the sealed-tube reactions.) The products were ground with a mortar and pestle in a He-filled drybox and then washed in air with methanol, water, and diethyl ether to remove the sodium halide and any unreacted starting reagents. The isolated products were then dried on a vacuum line. Reactions were also performed where excess red phosphorus was added to stoichiometric $InI_3 + Na_3P$ reaction mixtures. The phosphorus powder was ground into the sodium phosphide precursor before mixing with the InI_3 powder. The reactants were ignited and the products isolated in the manner described above.

Characterization. Powder X-ray diffraction (XRD) patterns were obtained on a θ–2θ drive Crystal Logic powder diffractometer with Ni-filtered Cu Kα radiation, scanning in steps of 0.02° 2θ at a rate of 10 s/step. These parameters were sufficient to allow detection of even minor contaminants. All precursors and products were identified and checked for purity by XRD. Scanning electron microscopy (SEM) was performed on a Cambridge SEM using a LaB_6 tip. The quantitative and qualitative elemental analyses were performed by energy-dispersive spectroscopy (EDS) using a Link AN10000 energy dispersive analyzer attached to the SEM. EDS was performed on various regions across the sample surface, using both area scans (at different magnifications) and point scans to determine regional homogeneity. Quantitative analyses were performed relative to single-crystal, thin-film standards of GaAs and InP prepared by molecular beam epitaxy. A 5× light microscope was employed for visible observations.

Solid-State NMR. Solid-state ^{31}P NMR studies were carried out at 121.6365 MHz, using a General Electric GN-300 spectrometer, equipped with a high-speed magic-angle spinning (MAS) NMR probe from Doty Scientific. ^{31}P MAS NMR spectra were recorded at spinning speeds around 8.5 kHz, with pulses of 4-μs length and 15-min relaxation delays. It was established that under these conditions the signal was not affected by saturation effects. Chemical shifts were referenced to 85% H_3PO_4. To assess the compositional purity of the samples, spin-counting experiments were carried out with commercial GaP (Alfa, 99.999% (metals basis)), prepared by liquid phase epitaxy, as the quantitation standard.

^{69}Ga NMR studies were carried out at 120.075 MHz using a General Electric GN-500 spectrometer. ^{69}Ga MAS NMR spectra were recorded at spinning speeds around 8.6 kHz, with a 2-μs pulse length and a 10-s relaxation delay. The commercial GaP sample served both as a chemical shift reference and as the reference standard for quantitative spin-counting studies.

Table I. Summary of Results

reactants	method	product(s)[a]
$AlI_3 + Na_3P$	bomb ignition	amorphous
	990 °C/42 h	AlP
$AlI_3 + Na_3As$	bomb ignition	amorphous
	220 °C/12 h	AlAs + Al + As
	550 °C/17 h	AlAs + As (trace)
$AlI_3 + Na_3Sb$	bomb ignition	AlSb + Al + Sb
	550 °C/12 h	AlSb + Sb + Al (trace)
	>600 °C/18 h	AlSb + Sb (trace)
$GaF_3 + Na_3P$	bomb ignition	GaP + P (red) + Ga (trace)
$GaCl_3 + Na_3P$	bomb ignition	GaP + P (red) + Ga (trace)
$GaI_3 + Na_3P$	bomb ignition	GaP + P (red) + Ga (trace)
	bomb ignition (8 mmol)	GaP + P (red) + Ga (trace)
	>220 °C/8 h	GaP + Ga (trace)
$GaI_3 + Na_3As$	bomb ignition	GaAs + Ga (trace)
	bomb ignition (8 mmol)	GaAs + Ga (trace)
	<570 °C/12 h	GaAs + As (trace)
	950 °C/8 h	GaAs
$GaI_3 + Na_3Sb$	bomb ignition	GaSb + Sb
	<600 °C/12 h	GaSb + Sb (trace)
$GaF_3 + Na_3Sb$	bomb ignition	GaSb + Sb (< from GaI_3)
$InI_3 + Na_3P$	bomb ignition	InP + In + InI_2 + P (red)
	<600 °C/12 h	InP + In + InI_2
	>600 °C/12 h	InP
$InF_3 + Na_3P$	bomb ignition	InP + In + impurity (trace)
$InI_3 + Na_3As$	bomb ignition	InAs + In + InI_2
	<600 °C/12 h	InAs + In + InI_2
	>600 °C/12 h	InAs + In
$InF_3 + Na_3As$	bomb ignition	InAs + In + impurity (trace)
$InI_3 + Na_3Sb$	bomb ignition	InSb + In + Sb
	550 °C/12 h	InSb + Sb (trace)

[a] Either NaI, NaCl, or NaF is a crystalline product formed in each of these reactions.

Results

The 13–15 materials were prepared by the solid-state precursor reaction

$$MX_3 + Na_3Pn \xrightarrow[\text{or (2) ignite}]{\text{(1) heat in sealed tube}} MPn + 3NaX \xrightarrow{\text{wash}} MPn \quad (1)$$

where M = Al, Ga, or In; X = F, Cl, or I; and Pn = P, As, or Sb. When the reaction mixtures were heated in sealed ampules, the products could be isolated as indicated in eq 1. Each reaction mixture had a threshold temperature for completion, and when heated above that temperature, the 13–15 product could be isolated with little or no elemental contamination or sodium halide detectable by XRD or EDS. The precursor reactions and conditions used to form the binary materials are summarized in Table I. While the large number of possible reactions and products

(16) *CRC Handbook of Chemistry and Physics*; Weast, R. C., Ed.; CRC Press: Boca Raton, FL, 1983.
(17) (a) Cahn, R. W. *Adv. Mater.* **1990**, *2*, 314. (b) Merzhanov, A. G.; Borovinskaya, I. P. *Dokl. Akad. Nauk SSSR (Engl. Transl.)* **1972**, *204*, 429. (c) Yi, H. C.; Moore, J. J. *J. Mater. Sci.* **1990**, *25*, 1159.
(18) (a) Munir, Z. A.; Anselmi-Tamburini, U. *Mater. Sci. Rep.* **1989**, *3*, 277. (b) Munir, Z. A. *Ceram. Bull.* **1988**, *67*, 342.
(19) Treece, R. E.; Macala, G. S.; Kaner, R. B. *Chem. Mater.* **1992**, *4*, 9.

represented by eq 1 could be achieved by sustained heating in sealed ampules (method 1), the products of the ignition reactions (method 2) frequently included other materials. The ignition reaction products (summarized in Table I) fell into three general categories: (a) crystalline 13–15's only; (b) crystalline 13–15's plus other materials; and (c) amorphous species.

GaP and GaAs. GaP and GaAs were the only 13–15 compounds which could be isolated as phase-pure polycrystalline powders by both of the reaction methods described in eq 1. The production of gallium phosphide and gallium arsenide from the ignition of GaI_3 and Na_3P and Na_3As has been described previously.[19] The GaP materials were XRD-pure, but small amounts of red phosphorus could be seen by optical microscopy with the amount of red phosphorus decreasing dramatically as the total amount of the reaction mixture was increased from 1.0 mmol (~550 mg) to 8.0 mmol (~4400 mg). It was suggested that the amount of red phosphorus decreased because the larger reaction mixture led to better insulation through an increase in the ratio of surface area to volume of the reaction mixture. Hence, there was an increase in total heat available to the reactants.

The qualitative change in the amount of visible red phosphorus led to further investigations on the effect of sample size (the amount of the reaction mixture) and heating on product quality. Three samples of GaP were synthesized from GaI_3 and Na_3P by methods 1 (1 mmol) and 2 (both 1.0 mmol and 8.0 mmol mixtures). Quantitative EDS analysis of the three products revealed that the Ga:P ratio was 1:1, within experimental errors, for each of the samples, regardless of the reaction size or method, and that composition of the powders was uniform across the surface. The lattice constants are a_0 = 5.454(1) Å and a_0 = 5.457(1) Å for the 1- and 8-mmol ignited samples, respectively, and a_0 = 5.456(1) Å for the heated material. These can be compared to a literature value of 5.448 Å.[20] Three samples of GaAs were also prepared in the same manner as described above for the GaP materials. In contrast to the case of GaP materials, there was some variation in the composition of the GaAs samples as measured by EDS. The 1.0-mmol ignition sample was consistently As rich with the Ga:As ratio ranging from 38:62 to 46:54, depending on the region examined. The 8.0-mmol sample showed regional inhomogeneity as well, but it varied from As rich (43:57), to ca. stoichiometric (51:49), to Ga rich (53:47). The bulk of the heated material was slightly Ga rich (53:47) with some metallic gallium spheres visible by SEM. The lattice constants of these materials are a_0 = 5.657(1) Å and a_0 = 5.659(1) Å for the 1- and 8-mmol samples, respectively, and a_0 = 5.658(1) Å for the heated compound. These lattice constants can be compared to a reported value of 5.6538 Å.[20]

When any of the gallium(III) halides were ignited with Na_3P, GaP was the only material detectable by XRD in the washed product. The isolated products were fine yellow powders, and representative XRD patterns are shown in Figure 1. The lattice constants are a_0 = 5.454(1) Å for the materials made from GaI_3 (I-GaP) and $GaCl_3$ (Cl-GaP) and a_0 = 5.455(1) Å for the compound made from GaF_3 (F-GaP). It can be seen by comparison of the signal-to-noise ratios and the peak shapes of the 331 lines at 76° 2θ that Cl-GaP is less crystalline than the GaP prepared from the other two precursors. There is, however, no appreciable difference between XRD patterns of the I-GaP and F-GaP materials.

The fact that XRD-pure GaP could be produced from each of the GaX_3 precursors made this system ideal for studying the effect of using different gallium halides on reaction initiation conditions. A reaction self-initiated within seconds when $GaCl_3$ was simply placed in contact with Na_3P. Therefore, it was not possible to thoroughly premix the $GaCl_3$ and Na_3P precursors before self-ignition. The reaction between GaI_3 and Na_3P could be initiated by grinding with a mortar and pestle but, for convenience, was typically ignited in a bomb with a hot filament. The reaction of the GaF_3 + Na_3P precursor mixture could not be initiated by grinding; the mixture could only be ignited by a hot wire. The initiation conditions for the GaX_3 + Na_3P series are summarized in Table II.

To assess the sample purity, quality, and crystallinity, solid-state ^{31}P and ^{69}Ga NMR spectroscopies were used. The results are summarized in Table III. Depending on preparation history, the ^{31}P resonances are found between −142.9 and −144.4 ppm, with half-height widths between 310 and 400 Hz for the various samples. These results are consistent with ^{31}P literature values for bulk GaP.[21] The broadening of the MAS NMR lines arises from distributions of isotropic chemical shifts and can serve as

(20) *Powder Diffraction File*; Joint Committee on Powder Diffraction Standards-International Center for Diffraction Data: Swarthmore, PA, 1986; File No. 12-191 (GaP) and File No. 32-389 (GaAs).

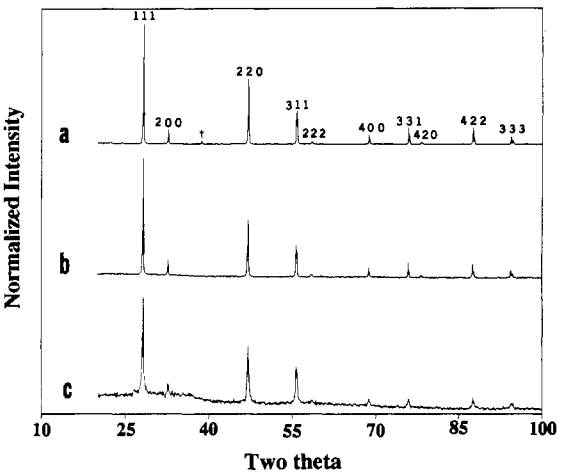

Figure 1. Powder XRD patterns illustrating the effect of the halide ligand on the crystallinity of GaP prepared from the ignition of 1-mmol mixtures of Na_3P and (a) GaF_3, (b) GaI_3, and (c) $GaCl_3$. The Miller indices of GaP and a trace of NaF (†) are indicated in the top pattern.

Table II. Summary of Initiation Conditions

GaX_3	mp (°C)	pnictide	dec (°C)	initiation conditions
$GaCl_3$	78	Na_3P	>550	stirring together
GaI_3	212	Na_3P	>550	grinding with mortar and pestle
GaF_3	>900	Na_3P	>550	heating with hot wire[28]

Table III. Solid-State ^{31}P and ^{69}Ga NMR Parameters: δ (Isotropic Chemical Shift, ±0.2 ppm), FWHM (Full Width at Half-Maximum, ±5 Hz), Percentage of Phosphorus Present in the Form of GaP, and Ga:P NMR Center Band Intensity Ratio Relative to That Measured in Commercial GaP

sample[a]	$\delta(^{31}P)$ (ppm)	^{31}P FWHM (Hz)	$\delta(^{69}Ga)$ (ppm)	^{69}Ga FWHM (Hz)	% P as GaP	Ga:P
GaP (Alfa, 99.999%)	−142.9	343	0.00	278	98.7	1.000
F-GaP no. 1	−143.4	353	1.09	307	96.2	0.783
F-GaP no. 2	−143.6	315	1.06	302	97.4	0.833
F-GaP HT	−144.2	343	1.19	287	93.7	0.900
I-GaP no. 2	−144.1	340	1.37	346	90.7	0.776
I-GaP HT	−144.4	324	1.43	324	86.4	0.724
Cl-GaP no. 1	−144.2	359	1.41	340	66.3	0.656
Cl-GaP no. 2	−144.4	364	1.39	372	63.2	0.633
Cl-GaP HT	−144.4	400	1.29	371	80.1	0.616

[a] X-GaP (where X is F, Cl, or I) designations indicate the GaX_3 precursor used to prepare the GaP, and HT indicates the annealed samples.

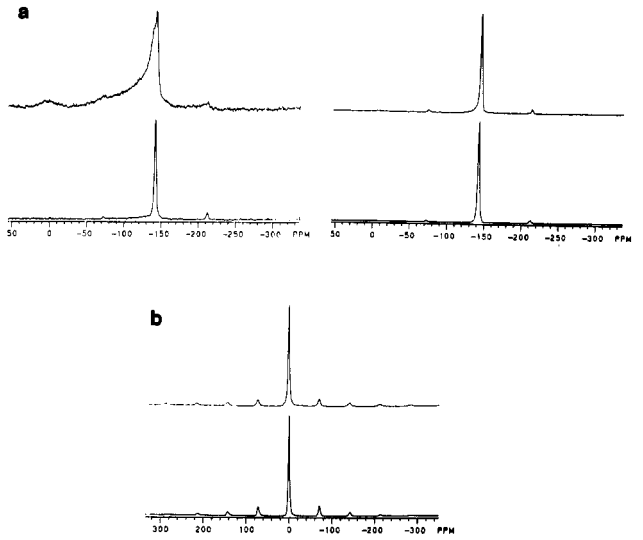

Figure 2. Representative solid-state NMR spectra comparing (top) polycrystalline GaP prepared from the ignition of GaI_3 and Na_3P and (bottom) commercial bulk GaP. In (a), 121.6365-MHz ^{31}P MAS NMR spectra are shown for two relaxation delays: 100 ms (left) and 900 s (right). In (b), 120.073-MHz ^{69}Ga MAS NMR spectra are shown for the same samples. Minor peaks symmetrically spaced around the sharp resonance are spinning sidebands.

a measure of crystalline disorder. The upfield shift is likely to be an electronic doping effect arising from intrinsic or extrinsic defects. Figure 2 compares the ^{31}P and ^{69}Ga NMR spectra of a typical sample prepared by rapid solid-state synthesis with those of bulk commercial GaP. The ^{31}P MAS NMR spectra also show evidence of several phosphorus-containing impurities: elemental (red) phosphorus (evident in some of these samples by optical microscopy) gives rise to a very broad background resonance. The spin–lattice relaxation time associated with this background feature is very short, so that its relative contribution to the signal can be enhanced by rapid pulsing (Figure 2a, left). The distinct T_1 difference between this species and GaP reveals the absence of spin diffusion and suggests that the P atoms giving rise to the sharp resonance (GaP) and those giving rise to the broad background are microscopically separated. However, this is not rigorous proof for the assumption that the broad feature is entirely due to elemental phosphorus impurities. We cannot rule out that part of this broad background belongs to strongly disordered phosphorus sites associated with defects or grain boundaries in GaP. Finally, several samples (particularly the Cl-GaP compounds) show an extra resonance near 0 ppm. This chemical shift suggests assignment to a phosphate-like species (perhaps $GaPO_4$), which may have arisen from oxidation of high-surface-area samples during washing. Furthermore, weak and as of yet unassigned features at −170 and −200 ppm are observed in some of the I-GaP and Cl-GaP samples, and the ^{31}P spin count reveals that the signal intensity per gram in most of the samples studied is only around 50% of that measured in bulk commercial GaP. The reasons for these observations are under investigation.

The ^{69}Ga MAS NMR line widths and chemical shifts show trends similar to those of the phosphorus resonance. Again, the spectral parameters of the F-GaP are closest to bulk commercial GaP, while the Cl-GaP samples show the largest differences. In addition, being a quadrupolar nucleus, the ^{69}Ga isotope is well-suited to probe the crystalline quality and the defect concentration relative to that of the commercial sample. For a spin $^3/_2$ nucleus such as ^{69}Ga three $\Delta m = \pm 1$ NMR transitions are expected. In perfectly cubic environments these three transitions are degenerate, resulting in one sharp peak only. In the presence of defects, however, an electric field gradient is present at the gallium sites, which interacts with the ^{69}Ga nuclear electric quadrupole moment and affects the Zeeman energy levels. As a result, only the central $^1/_2 \rightarrow -^1/_2$ transition remains unperturbed, whereas the locations of the other two resonances become orientationally dependent.[22] Consequently, in a polycrystalline material these transitions give rise to broad powder patterns, which become a spinning sideband manifold under MAS conditions.[23] This is illustrated in Figure 2b, which shows a representative ^{69}Ga MAS NMR spectrum of GaP made by rapid SSM. In reality, spinning sidebands are always observed, even in the purest and crystallographically most perfect GaP samples, because there is always a finite concentration of intrinsic defects, affecting gallium atoms as far as 30 Å apart.[24] Due to this far-reaching effect of distance, a distribution of quadrupole splittings is expected, the details of which are difficult to model.[23] Regardless of the electric field gradient magnitude, however, such splittings decrease the intensity of the dominant central line observed in the MAS NMR spectra. It is further expected that this intensity loss correlates with the defect concentration. We have quantified this signal loss by detailed spin-counting studies on weighed samples, comparing both the ^{31}P and the ^{69}Ga signal intensities with those of commercial bulk GaP. Table III summarizes the Ga:P signal intensity ratios determined in this fashion relative to that in commercial GaP (set arbitrarily to unity). Note that for all of the samples prepared by metathesis reactions this ratio is smaller than 1, indicating that the defect concentration is higher than in commercial GaP. Additional experiments and further detail on the use of solid-state NMR as an analytical tool for 13–15 compounds will be presented elsewhere.[25]

Other 13–15 Compounds. The remaining metal(III) halide and sodium pnictide ignition reactions yielded either the appropriate 13–15 compound with one or both of the constituent elements and/or lower metal halides or an amorphous material (in the case of AlP). One example which produced excess elements as well as the desired 13–15 product was the ignition reaction between AlI_3 and Na_3As. The ignition products included AlAs, NaI, and Al and As metals, as shown in eq 2. When the unwashed

$$AlI_3 + Na_3As \xrightarrow{\text{ignite}} AlAs + NaI + Al + As \xrightarrow[\text{(2) wash}]{\text{(1) 1000 °C/8 h}} AlAs \quad (2)$$

ignition products were subsequently heated in a sealed silica ampule at 1000 °C for 8 h, phase-pure AlAs was isolated. Powder XRD patterns of washed powders of the direct ignition products and the postignition heated AlAs are presented in Figure 3.

A second example of a reaction that produced a crystalline 13–15 along with additional species is the combination of InI_3 and Na_3P. As shown in Table I, both the ignition and controlled heating (below 600 °C) of an indium(III) iodide and sodium phosphide precursor mixture resulted in InP, indium metal, and InI_2. When the precursor mixture was heated above the threshold of 600 °C, the only material detectable by XRD was InP. Powder XRD patterns of InI_3 + Na_3P reaction products are shown in Figure 4.

The effect of adding excess red phosphorus to InP precursor mixtures was also investigated. To 596 mg (1.0 mmol of precursor mixture; $x = 0$) of InI_3 + Na_3P, was added red phosphorus in

(21) (a) Nissan, R. A.; Vanderah, T. A. *J. Phys. Chem. Solids* **1989**, *50*, 347. (b) McDougall, J. E.; Eckert, H.; Stucky, G. D.; Herron, N.; Wang, Y. *J. Am. Chem. Soc.* **1989**, *111*, 8006.

(22) Cohen, M. H.; Reiff, F. *Solid State Physics*; Seitz, F., Turnbull, D., Eds.; Academic Press: New York, 1958; Vol. 5, p 321.

(23) Han, O. H.; Timken, H. K. C.; Oldfield, E. *J. Chem. Phys.* **1988**, *89*, 6046.

(24) (a) Rhoderick, E. H. *Philos. Mag.* **1958**, *3*, 545. (b) Rhoderick, E. H. *J. Phys. Chem. Solids* **1958**, *8*, 498. (c) Carlos, W. E.; Bishop, S. G.; Treacy, D. J. *Appl. Phys. Lett.* **1986**, *49*, 528. (d) Carlos, W. E.; Bishop, S. G.; Treacy, D. J. *Phys. Rev. B* **1991**, *43*, 12,512.

(25) Franke, D.; Treece, R. E.; Kaner, R. B.; Eckert, H. *Anal. Chim. Acta*, in press.

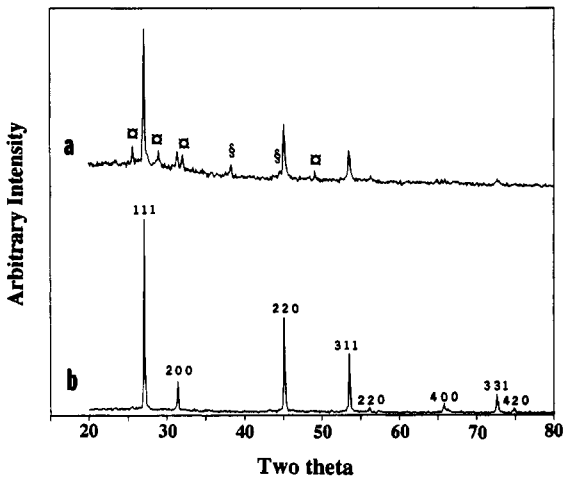

Figure 3. Powder XRD patterns of the products of the $AlI_3 + Na_3As$ reaction by (a) ignition and (b) sustained heating. Arsenic (O) and aluminum (§) impurities are labeled in (a), with the Miller indices of AlAs indicated in (b).

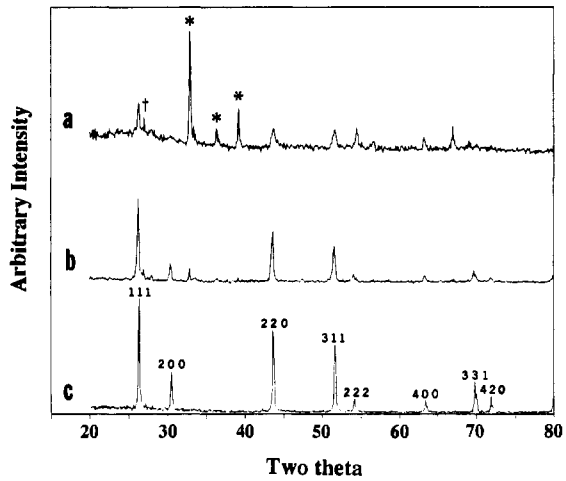

Figure 4. Effect of heating above the reaction threshold illustrated by powder XRD patterns of the washed products of $InI_3 + Na_3P$ reactions by (a) ignition and sustained heating at (b) 550 °C and (c) 650 °C. Indium (*) and InI_2 (†)[26] impurities are labeled in (a), and the Miller indices of InP are indicated in (c).

20-mg (x = 0.65 mmol phosphorus equivalent), 40-mg (x = 1.3 mmol phosphorus equivalent), and 100-mg (x = 3.2 mmol phosphorus equivalent) allotments to the precursor mixtures, as shown in eq 3. Powder XRD patterns of the ignition products

$$InI_3 + Na_3P + x(\text{red})P \xrightarrow[\text{(2) wash}]{\text{(1) ignite}} InP + InI_2 + In + NaI \quad (3)$$

of these reactions are displayed in Figure 5, along with a pattern of a sample where red phosphorus was not added. As the amount of excess phosphorus was increased, the diffraction lines associated with InP increased relative to the highest intensity lines of indium metal and InI_2,[26] indicating that the amounts of the crystalline impurities were decreasing relative to that of the product InP.

The product isolated from one ignition reaction was amorphous, while extended heating of an identical precursor mixture resulted in a polycrystalline powder of the desired material. When a reaction mixture of AlI_3 and Na_3P was ignited, the washed products were amorphous to X-rays (Figure 6a). When a similar reaction mixture was heated in a sealed silica ampule at 1000 °C

(26) InI_2 has been identified in the products of the unwashed samples, but the peaks in the XRD patterns of the washed materials, denoted as InI_2*, result from the reaction $InI_2 + H_2O$.

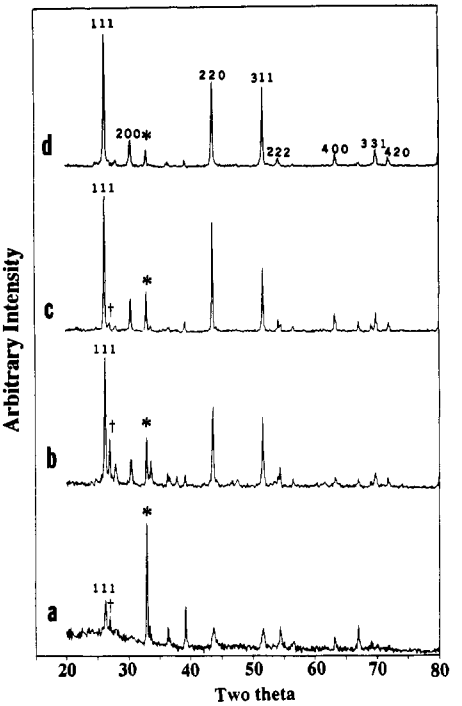

Figure 5. Effect of increasing addition of red phosphorus to InP precursor reactions illustrated by the lower impurity levels found in XRD patterns of the washed ignition products of $InI_3 + Na_3P + xP$(red) reactions: (a) x = 0; (b) x = 0.65; (c) x = 1.4; (d) x = 3.6. The most intense peaks of indium (*), InI_2 (†),[26] and InP (111) are labeled for comparison. The Miller indices of InP are indicated in (d).

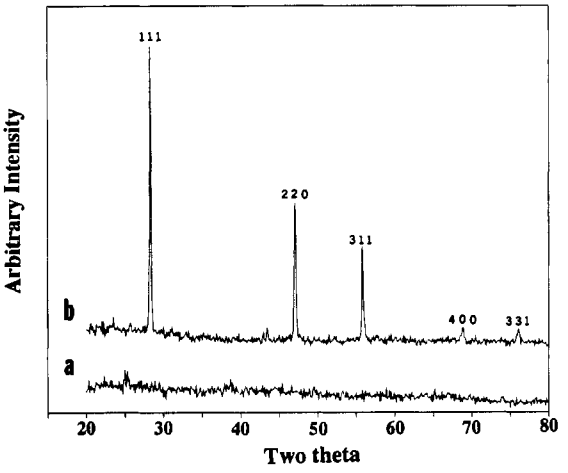

Figure 6. Powder XRD patterns of the products of $AlI_3 + Na_3P$ reactions by (a) ignition and (b) sustained heating at 990 °C for 42 h. The Miller indices of AlP are indicated in (b).

for 42 h, the washed products were identified exclusively as AlP (Figure 6b).

Discussion

Heating the appropriate precursors in sealed ampules, as shown in eq 1, allows for the production and isolation of XRD- and EDS-pure, fine, single-phase 13–15 powders through a general synthetic method. This method overcomes many of the difficulties associated with traditional, high-temperature elemental reactions.[2,3] While the sustained heating reactions yield phase-pure materials, several of the ignition reactions leave elemental species and lower halides in the products. In an effort to understand why some of the materials produced in ignited reactions differ from the products observed following prolonged heating, a discussion of initiation conditions, reaction intermediates and product formation, and the role of T_{ad} and reaction size (i.e., the ratio of

surface area to volume of the reaction mixture) in self-annealing within the rapid SSM processes is needed.

Initiation Conditions. Ignition of the self-sustaining metathesis reactions requires that the initial surface reaction generate sufficient heat in the early steps to overcome the overall reaction barrier of the bulk mixture. The major factors influencing the initial surface reactions are the precursor melting/boiling points. Vaporization, melting, and/or decomposition of the lowest melting/decomposing precursor destabilizes the reactant lattices, allows for more rapid atomic diffusion, and increases surface contact, thereby initiating the reaction.[9-14]

Many of the 13–15 metathesis reactions self-initiate while others require some thermal input. The initial step in the metal iodide and metal chloride precursor reactions appears to be melting and/or vaporization of the metal halide precursors. Precursor melting is followed by production of the sodium halide byproduct, with subsequent formation of the 13–15 products occurring within the molten reaction flux. GaI_3, for example, solidifies as a high-vapor-pressure, dimeric molecular solid[27] (mp of 212 °C, sublimation at >345 °C),[16] and reactions between it and Na_3X can be initiated by grinding with a mortar and pestle. The grinding action apparently provides sufficient heat to melt and/or vaporize some GaI_3, thereby increasing surface contact allowing for initiation. Isostructural $GaCl_3$ melts at 78 °C and has a relatively high vapor pressure at room temperature; reactions between it and Na_3P self-initiate within seconds upon mixing. Reactions with GaF_3, however, do not self-ignite. This is likely due to the three-dimensional network structure[27] of GaF_3 with its high sublimation point (950 °C),[16] which is greater than the temperature produced by the hot filament (~850 °C).[28] It appears that decomposition of the pnictiding agent (e.g. Na_3P, decomposition at >600 °C)[16] destabilizes the precursor lattice sufficiently to enable initiation of the reaction between the metal fluoride and sodium pnictide. The absence of any appreciable room-temperature vapor pressure from either the sodium pnictides or the metal fluorides explains the observations of no self-initiating reactions between the fluoride and pnictide precursors.

Reaction Intermediates and Product Formation. Once initiated, these ignited precursor reactions are highly exothermic and quite rapid. The heat generated in the self-sustaining processes is sufficient to vaporize or melt the reactants and byproducts, thereby overcoming solid-state diffusion barriers to reaction and producing a molten flux. The molten halide flux allows for rapid formation of more products and byproducts, which in turn generates more heat. The rapid heating is followed by rapid cooling of the flux, which can be seen as kinetically quenching any unfinished diffusion/reaction processes. Since the reactions are so brief, it is not possible to directly examine the intermediate stages by traditional solid-state chemistry techniques (e.g., XRD), but it is very likely that the materials quenched in the products reflect intermediate species. It is necessary, therefore, to consider reaction processes on the basis of examination of the products.

The presence of extraneous species in the ignition reactions indicates that these processes are not going to completion but instead are being quenched. While it is possible that the excess elemental species may arise from the reversible decomposition of the rapidly-formed 13–15 product, it seems unlikely. It is clear from Table I that, given sufficient heat and time, almost any combination of metal halide and sodium pnictide will produce exclusively the desired 13–15 product and sodium halide byproduct. While the complete reactions are different for methods 1 and 2, both processes begin with precursor ignition. Observation of the sealed-tube reactions reveals that at some critical temperature the precursor mixture ignites within the tube, indicating that the initial steps in both methods involve reactant ignition. The difference between the two approaches is that for method 1 the continued heating, following ignition, provides additional thermal energy to the reacting species, allowing for further diffusion and subsequent reaction. As stated earlier, the ignition products fell into three general categories: (a) crystalline 13–15's only; (b) crystalline 13–15's plus other compounds; and (c) amorphous materials. The ignition products provide a snapshot of the reaction process, with each case providing additional information.

The amorphous materials provide insight into the earliest steps of the reaction. Under ignition conditions, crystalline AlP does not form at all. However, given sufficient time (42 h) at a high temperature (1000 °C), aluminum phosphide is formed from AlI_3 and Na_3P (Figure 6), indicating that AlP is the thermodynamic product of this reaction. When AlI_3 and Na_3P are ground together but not ignited, an XRD pattern of the unwashed products reveals the formation of partially crystalline NaI and the complete absence of any precursor or AlP reflections. At this point in the reaction process all long-range structural order, except for the beginning of NaI formation, has been destroyed. The amorphous materials could possibly be AlP, aluminum, lower aluminum halides, and/or phosphorus, but whatever the amorphous intermediates are, they clearly require additional heating to react further or to crystallize or both.

The processes resulting in crystalline 13–15's and other materials provide insight into the steps following the production of the amorphous intermediates. The reaction of InI_3 with Na_3P is a good example. The products of the ignition of InI_3 and Na_3P, along with InP and NaI, include indium metal, reduced indium iodide (InI_2), and red phosphorus (Figure 5). The presence of elemental species and InI_2 suggests that the reaction process involves the reduction of InI_3 and the oxidation of Na_3P within the flux. While it is likely that much of the product formation occurs through a metathetical (simple ion exchange) pathway, it appears that the oxidizing power of the iodide ligands is not sufficient to prevent reduction of some In^{3+} by P^{3-} within the reaction flux. In fact, some redox occurs in all of the InI_3 + Na_3Pn precursor reactions, as evidenced by the presence of elemental indium or pnictogen, or both, in the products. In these cases, neither redox nor the subsequent reaction between the elements goes to completion.

In order to more fully investigate the role of neutral elements in InP precursor reactions, red phosphorus was added to the reaction mixture. As can be seen in Figure 5, the effect of adding elemental phosphorus to the reaction mixture is to reduce the amount of metallic indium and InI_2 in the products. The presence of excess elemental phosphorus in the reaction mixture appears to facilitate the conversion of InI_3 to InP. If redox is involved in the reaction process, and the formation of some InP occurs through reaction between In^0 and P^0, it seems reasonable that the presence of excess P^0 would favor the formation of InP. The likelihood of InP formation is increased through reducing the diffusion path length between phosphorus and the reactive indium centers. It is also likely that the presence of reduced metal halides (i.e., InI_2) in the reaction flux serves to promote 13–15 production by preventing the formation of an inhibiting layer, a thin skin of product around reacting metal particles.[6]

The role of the halide ligand in the indium reactions was examined further with InF_3. The presence of indium metal in the InF_3 + Na_3Pn ignition reaction products indicates that a redox pathway may also occur with the fluoride as well as the iodide precursors. Apparently, since indium readily occupies oxidation states of 0, +1, and +3, even the strong oxidizing power of the fluoride ligand does not completely stabilize the In^{3+} against reduction in the presence of the pnictide anions.

Self-Annealing and T_{sa}. An important aspect of these ignition reactions is self-annealing, the process whereby the products are

(27) Wells, A. *Structural Inorganic Chemistry*, 5th ed.; Clarendon Press: Oxford, England, 1986.
(28) The temperature of the filament (~850 °C) was determined with a K-type thermocouple and by optical pyrometry.

crystallized by the heat remaining in the flux. Three major factors affecting the amount of heat available to the reacting species are the enthalpy of the reaction, the adiabatic temperature, and the degree of insulation. Whereas the reaction enthalpies are roughly equivalent, T_{ad} varies considerably depending on the metal–halide ligand, and the degree of insulation is related to the mass of the reaction. The following section discusses efforts to isolate and examine each of the thermal factors.

The relationship among ΔH_{reacn}, T_{ad} and crystallinity was investigated by studying the GaP products of the reactions

$$GaX_3 + Na_3P \rightarrow GaP + 3NaX \qquad (4)$$

where X = F, Cl, or I. The enthalpy of the precursor reaction used to produce GaP from GaF_3 and Na_3P (eq 4), calculated from Hess' law, is −124 kcal/mol.[16,29,30] The production of 3 mol of byproduct NaF produced accounts for 95% of the theoretical heat of product formation. This serves as a potent driving force and determines the theoretical maximum reaction temperature, T_{ad}. The adiabatic temperature calculated for the reaction between GaF_3 and Na_3P is 1695 °C, corresponding to the boiling point of NaF.[18] In fact, when X = I, the ΔH_{reacn} = −138 kcal/mol, and when X = Cl, the ΔH_{reacn} = −160 kcal/mol. In each of the GaP reactions (shown in eq 4), T_{ad} corresponds to the boiling point of the sodium halide.[16,29,30] T_{ad} represents a theoretical upper limit of the temperatures these metathesis reactions may actually attain, and temperatures even approaching these values could certainly lead to self-annealing of the reaction products.

Since annealing generally affects the crystallinity of a material, the GaP samples produced in the $GaX_3 + Na_3P$ (X = F, Cl, I) series were characterized by both XRD and solid-state NMR. It is clear from the XRD patterns (Figure 1) that the crystallinity of the GaP products prepared from the GaF_3 (F-GaP) and the GaI_3 (I-GaP) precursors is greater than that prepared from the $GaCl_3$ (Cl-GaP) material. Using solid-state NMR, these differences can be discussed on a more quantitative basis. All solid-state NMR parameters measured in this study consistently show an increase in defect concentration and a decrease in crystalline quality from F-GaP to I-GaP to Cl-GaP. One possible explanation for this ordering relies on the maximum temperatures to which each product is exposed. In the case of F-GaP, T_{ad} provides sufficient heat to *melt* both products and begin to vaporize the NaF (see Figure 7). Therefore, it is theoretically possible that the GaP product (mp = 1520 °C) is solidified from the *liquid phase* in a NaF flux.[30a] Sodium fluoride is the only byproduct halide which has a melting temperature greater than that of GaP.

While it is clear why F-GaP might be more crystalline than I-GaP and Cl-GaP, an explanation of why I-GaP is more crystalline than Cl-GaP requires an examination of factors other than T_{ad}. The T_{ad} calculated for the preparation of Cl-GaP (T_{ad} = bp_{NaCl} = 1413 °C)[16] is greater than that determined for I-GaP (T_{ad} = bp_{NaI} = 1304 °C)[16] (Figure 7). Solely on the basis of T_{ad}, the reason for the observed differences is not apparent; however, an examination of the initiation conditions reveals that the Cl-GaP reactions self-initiate before the precursors are thoroughly mixed and the heat generated in the initial processes melts the remaining unreacted $GaCl_3$. These reactions are effectively carried out in a pool of liquid $GaCl_3$ (78 °C < T_{flux} < 212 °C).[31] The I-GaP reactants, however, are mixed very well and the reaction

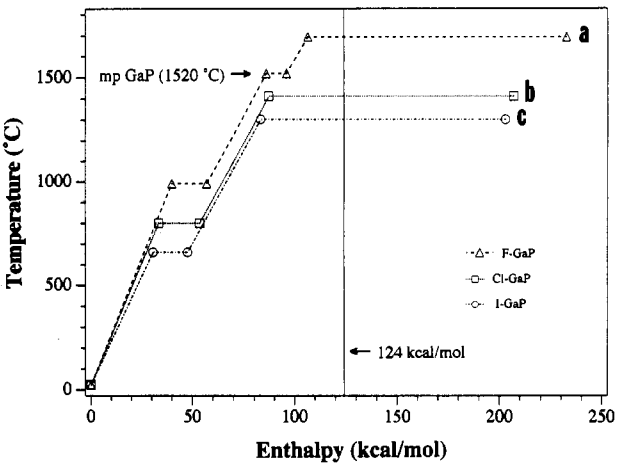

Figure 7. Plot of temperature versus enthalpy calculated for the products formed in the reactions between Na_3P and (a) GaF_3, (b) $GaCl_3$, and (c) GaI_3. The value for the heat released (124 kcal/mol) by reaction a is indicated by the vertical line.

is essentially instantaneous. The I-GaP and F-GaP reactions are closer to adiabatic processes and therefore have a much greater chance of approaching T_{ad}. Therefore, it is likely that the low reaction temperatures experienced by Cl-GaP lead to less crystalline products than observed for either F-GaP and I-GaP.

Self-Annealing and Reaction Size. Whereas the preceding section examined the role of ΔH_{reacn} and T_{ad} in self-annealing, this part discusses the effects of insulation. Two of the assumptions behind the calculation of T_{ad} are that the ignition reactions are essentially instantaneous and that there is relatively little heat lost to the surroundings. It is expected that larger reaction mixtures, with the correspondingly smaller ratios of surface area to volume, will better insulate the reactants, leading to both increased phase purity and crystallinity. The preparation of GaP and GaAs from GaI_3 and Na_3Pn precursors is used to study the effect of the mass of the reaction mixture (referred to as simply reaction size) because these processes are the fastest ($t \sim$ ms) of the 13–15 preparations and, therefore, closest to ideal adiabatic conditions.[32] Even though the amount of red phosphorus in the I-GaP products is shown to decrease with increasing reaction size,[19] the quality of the I-GaP samples appears to be independent of the reaction method and size. The lattice parameters (XRD), compositions (EDS), and crystallinities (NMR and XRD) are comparable for the three samples prepared by method 1 (1 mmol) and method 2 (both 1 and 8 mmol), indicating that for GaP insulation effects appear to be minimal.

This is contrasted by the three analogous GaAs samples. While the lattice constants of the three GaAs samples were similar, the composition and homogeneity were shown to vary considerably. Since the lattice constants arise from crystalline regions within the sample, and those values correspond to the reported lattice constant of GaAs, the large amount of excess arsenic in the 1 mmol GaAs material may be in the amorphous phase. The presence of amorphous arsenic together with crystalline, stoichiometric GaAs could account for the observed results. For the GaAs reactions, the effect of increasing the amount of reactants or heating the precursors in a sealed tube profoundly affects the amorphous arsenic. The 8-mmol ignition reaction product is inhomogeneous from region to region, but in contrast to the 1-mmol sample, the distribution centers about 50:50. In this case the added heat leads to a greater incorporation of arsenic into the sample and less excess amorphous arsenic to be detected by EDS. The observation that the sample prepared at 570 °C is exclusively gallium rich suggests that the continued heating may have sublimed away any amorphous arsenic remaining on

(29) *JANAF Thermochemical Tables*, 3rd ed.; Lide, D. R., Jr., Ed.; American Chemical Society and American Institute of Physics, Inc.: New York, 1985.

(30) (a) Kubaschewski, O.; Alcock, C. B. *Metallurgical Thermochemistry*, 5th ed.; Pergamon Press, Inc: New York, 1979. (b) *Lange's Handbook of Chemistry*, 13th ed.; Dean, J. A., Ed.; McGraw-Hill: New York, 1985.

(31) The effect of NaCl on the flux temperature is to lower it to 62 °C up to about 15 mol % NaCl. Even up to 50 mol % NaCl, the flux would remain below 250 °C. A phase diagram and other data on the $GaCl_3$–NaCl flux are given in: *J. Phys. Chem. Ref. Data* **1975**, *4*, 1033.

(32) High-speed photography has been used to observe similar ignition reactions, revealing that the peak of heat output occurs within 120 ms.[12]

the surface after product formation, and the presence of metallic gallium spheres indicates that a net loss of arsenic may have led to the observed gallium islands.

Conclusions

Solid-state metathesis (SSM) reactions are an effective synthetic route to 13–15 compounds. A wide range of phase-pure 13–15 materials can be synthesized by heating solid-state precursors in evacuated, sealed tubes. The precursor mixtures can also be ignited, but the products of these rapid self-sustaining reactions may include elemental and/or metal halide contaminants. On the basis of a study of the products of ignition processes, it has been suggested that these SSM reactions proceed through both a metathetical (double ionic exchange) and an elemental pathway. The elemental model requires that a redox reaction between M^{3+} and Pn^{3+} occur at some point in the ignition process. The reactions are initiated by a phase change in one of the precursors, whereupon sodium halide formation begins. At this point, an amorphous intermediate forms and subsequent reaction between the remaining elements occurs as long as there is sufficient heat. The ignition reactions have only the heat generated by product formation, whereas the sustained heating processes have additional thermal energy provided by a furnace. Each precursor mixture has threshold temperature and time requirements for completion.

Since the elemental pathway suggested for the 13–15 reactions requires redox between the metal and the non-metal, we have begun studies involving metals that are inherently more stable at fixed oxidation states than the group 13 elements, such as alkaline-earth (2+) and lanthanide (3+) metals. These metals would be expected to be more easily stabilized than the group 13 metals in the presence of a powerful reducing agent, possibly leading to an ionic pathway for alkaline-earth-metal or rare-earth-metal halide SSM reactions. We are also investigating the synthesis of mixed-metal and mixed-pnictide ternary III–V materials such as $Al_xGa_{1-x}As$ and GaP_xAs_{1-x}.

Acknowledgment. The authors gratefully acknowledge Dr. Philippe R. Bonneau and Dr. John B. Wiley for their participation in fruitful discussions of this research. This work was supported by the National Science Foundation and by a David and Lucile Packard Foundation Fellowship in Science and Engineering (R.B.K.). Financial support for the NMR experiments was provided by NSF Grant DMR-8913738 (H.E.).